Multielectron Effects in Charge Asymmetric Molecules Induced by Asymmetric Laser Fields

V. Tagliamonti, H. Chen, and G. N. Gibson
Department of Physics, University of Connecticut, Storrs, Connecticut 06269, USA
(Received 20 September 2012; published 14 February 2013)

Using a 45 fs pump pulse at 800 nm, a wave packet is created in a charge asymmetric dissociation channel of iodine, $I_2^{2+} \rightarrow I^{2+} + I^{0+}$ (2,0). As the molecule dissociates, a two-color ($1\omega 2\omega$) probe pulse is used to study the dynamics as a function of internuclear separation R. We find a critical region of R in which there is spatially asymmetric enhanced ionization of the (2,0) channel to a counterintuitive (1,2) channel. In this region the I^{0+} is ionized such that one electron is released to the continuum and another is transferred to the I^{2+} resulting in $I^{0+} \rightarrow I^{2+}$ and $I^{2+} \rightarrow I^{1+}$. At larger R, the ionization is consistent with simple one-electron ionization in a double well where $I^{0+} \rightarrow I^{1+}$. We find qualitative agreement between simulations and experiment further highlighting the importance of multielectron effects in the strong-field ionization of molecules.

DOI: 10.1103/PhysRevLett.110.073002 PACS numbers: 33.80.Rv, 32.80.Rm, 42.50.Hz

The interaction of molecules with a strong laser field can lead to interesting nonperturbative effects such as inner-orbital ionization [1–6], high-harmonic generation (HHG) [7–9], enhanced ionization (EI) [10–16], and charge asymmetric dissociation (CAD) of ionic fragments [17–19]. The CAD channels are particularly interesting as they indicate a high degree of electronic excitation over the ground-state charge symmetric dissociation channels [17], involve electron charge transfer and electron rearrangement [20–24], and have been used to demonstrate theories of EI and electron localization (EL) [12]. Further, the ion fragments produced through CAD exhibit spatial asymmetry (SA) in two-color, asymmetric $1\omega 2\omega$ laser fields [25–28]. This is significant because it allows us to directly observe charge transfer interactions which may otherwise go unnoticed.

Charge transfer in ionization processes has proved to be an important and unavoidable mechanism in strong field physics. The intense laser field can cause field-induced charge transfer between the nuclei and result in a strong electron-electron correlation [21]. It has been shown that charge transfer is possible between the symmetric and asymmetric states of even-charged diatomic molecules [29]. Further, upon ionization by a strong field the ionized electron may still interact with the parent ion and studying the amplitude and phase of this interaction has led to significant progress in understanding HHG [30,31] and in turn, molecular structure and electronic rearrangement [9,24]. For diatomics, the single-active-electron approximation has often been used as a first step in characterizing ionization, but the application to more complicated multielectron polyatomic molecules is unlikely to result in an accurate model [32,33]. As such, studying charge transfer in simpler systems like diatomics is an important step in understanding multielectron dynamics not only in ionization and dissociation, but in applications of attosecond physics and HHG.

In this work, we study the R dependence of charge transfer through the ionization of the (2,0) to (2,1) dissociation channel in I_2 [throughout this paper (n, m) designates the $I_2^{(n+m)+} \rightarrow I^{n+} + I^{m+}$ dissociation channel and indicates if the charge is on the left (n) or the right (m) atom]. In a symmetric (single color) field it would not be clear if the I^{0+} were simply ionized to I^{1+} [Fig. 1(a)] or if there was an electron rearrangement with ionization, where $I^{0+} \rightarrow I^{2+}$ and $I^{2+} \rightarrow I^{1+}$ [Fig. 1(b)]. Schematically, these different ionization pathways are described by Eq. (1):

$$\begin{array}{ccccc} & & A & & B \\ (0,2) & \Rightarrow & (1,2) & \leftarrow & \\ & \Rightarrow & (2,1) & \leftarrow & (2,0). \\ & & B & & A \end{array} \tag{1}$$

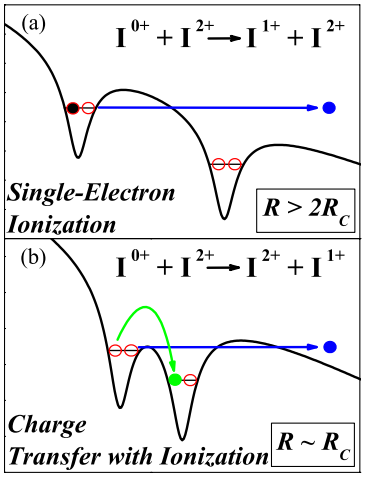

FIG. 1 (color online). One-dimensional double-well potential schematic showing the (a) single-electron ionization and (b) ionization with charge transfer processes near R_c and $2R_c$. The initial charge state (0,2) has two electrons in the upfield well so that the upfield atom has a 0^+ charge and the downfield ion has a 2^+ charge. The straight arrow indicates ionization and the curved arrow indicates charge transfer of the electron which occurs near R_c and is suppressed at larger R.

With symmetric fields, the (1,2) and (2,1) signals will always be equal, providing no indication of the relative strengths of the single-electron ionization (A) and charge transfer with ionization (B) mechanisms in Eq. (1). However, a $1\omega 2\omega$ field can preferentially ionize one well over the other, enhancing, for example, the double arrows over the single arrows in Eq. (1), immediately revealing the relative strength of the two processes.

An added complication is that molecular ionization in a strong field is also sensitive to the laser pulse duration, as a molecule will expand at different rates depending largely on its mass. Although CAD has been seen with long and short pulses [19,34], in both light [18,27] and heavy molecules [17,20], the R dependence of a process cannot be seen directly if ionization and dissociation occur at the same time during the laser pulse. For this reason, we chose to study I_2 in a pump-probe configuration.

In previous experiments [28], we studied SA in the *production* of the (2,0) CAD channel in I_2 as a function of internuclear separation R in a $1\omega 2\omega$ field. We found that while the (2,0) channel is produced at R_e, there is no SA. As the molecule dissociates from R_e, the SA increases reaching a maximum around R_c and drops off at larger R. These results would appear to support recent measurements in N_2 [27], where both the (2,0) and (2,1) channels showed SA. While the experiments performed in I_2 are time resolved and the measurements described for N_2 are not, there are still two problems. We have shown [34] that there is no expansion of the N_2 molecule to R_c until *after* N_2^{2+} is produced and therefore the (2,0) must be produced near R_e. Also, SA in (2,1) was not seen in I_2. Thus, SA cannot result from the spatially asymmetric *production* of (2,0) at R_c in N_2.

To resolve these issues, we study the possibility of SA in the *depletion* of the (2,0) channel as a function of R in I_2 [28]. If depletion occurs, SA in N_2 could be explained by the spatially symmetric (SS) production of (2,0) at R_e and SA depletion at R_c as the N_2^{2+} molecule expands on the (2,0) potential energy curve during the laser pulse. Any SA depletion of (2,0) must appear as SA enhancement in (2,1). In fact, the depletion of (2,0) in I_2^{2+} has been observed and used to demonstrate theories of one-electron EI at R_c [12]. In the simplest interpretation, the neutral atom is ionized to I^{1+} and, if done so with an asymmetric laser field, both the (2,0) and (2,1) channels would show SA but in opposite directions (based on the direction of the I^{2+} ion). Since the (2,0) and (2,1) channels in N_2 show the same direction for the asymmetry [27], either depletion is not the mechanism for the SA, or the EI experiment has a more subtle interpretation than previously thought. We will show that, indeed, the (2,0) channel can be depleted asymmetrically, the (2,1) channel does show SA, and that, at R_c, two-electron charge transfer is so strong that the induced asymmetry in the (2,1) channel is in the counterintuitive direction [in the context of depletion and Fig. 1(b)] and, thus, consistent with the directions observed in N_2 [27]. These conclusions are supported by time-dependent calculations of two electrons in a double-well potential.

The experiments are performed with a Ti:sapphire laser system (Spectra-Physics) at a 1 kHz repetition rate producing up to 800 μJ per pulse in 45 fs with a central wavelength of 800 nm. The beam is split to allow for pump-probe measurements. Both the pump and probe pulses are linearly polarized parallel to the time of flight (TOF) axis. The 800 nm pump pulse intensity is 2.0×10^{14} W/cm^2 and the $1\omega 2\omega$ probe intensity is 1ω: 6.5×10^{13} W/cm^2 and 2ω: 1.6×10^{13} W/cm^2. The $1\omega 2\omega$ pulse is produced by frequency doubling the 800 nm (1ω) beam in a 250 μm-thick β-barium borate (BBO) crystal and spatially separating the two colors in a Mach-Zehnder interferometer (details in Ref. [28]). To produce the maximum field asymmetry, the energies of the probe pulses are set at a 4:1 1ω:2ω ratio. The relative phase ϕ between the two pulses is stable to within 5°. The beams are focused by a spherical silver mirror inside an ultrahigh vacuum chamber with a base pressure of 10^{-9} torr. Iodine gas is effusively leaked into the chamber at room temperature to a pressure of 10^{-7} torr. The I^{2+} ion signals are detected with a Wiley-McLaren [35] TOF spectrometer. We record pump-probe TOF spectra for two phases of the $1\omega 2\omega$ field differing by π as well as the single pulse $1\omega 2\omega$ TOF spectrum.

A typical TOF data set for a single $1\omega 2\omega$ phase is shown in Fig. 2. The pump pulse launches dissociating wave packets in the (2,0) channel. As the molecule dissociates, the time-delayed probe pulse further ionizes (2,0) to (2,1). This ionization appears as "tracks" in the TOF spectrum from about 100 to 450 fs in a region where the kinetic energy release (KER) is between the (2,0) and (2,1)

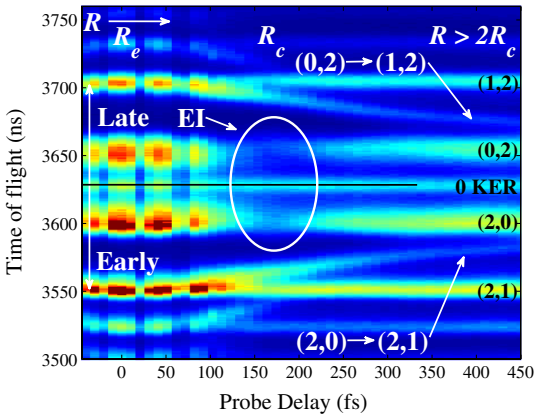

FIG. 2 (color online). Time of flight spectrum for I^{2+} at a single phase of the $1\omega 2\omega$ field as a function of probe delay with a step size of 10 fs. The three regions of R correspond approximately to R_e (0 fs), R_c (120–220 fs), and $R > 2R_c$ (~350–450 fs). The coherent structure from −50 fs to 100 fs is due to the interference of the pump and probe pulses near zero time delay.

channels observed with a single pulse [36]. The (2,1) KER decreases as the probe delay increases. There is a region of EI of (2,0) from around 120 fs to 220 fs in which the molecule passes through R_c. Here, the (2,0) channel is depleted by approximately 50% relative to the asymptotic population observed at large time delays. The depletion reaches a maximum at ~170 fs, consistent with the first observation of EI in I_2 [12] and subsequent observations [19,36]. Starting at about 100 fs delay, there is an enhancement of the (2,1) population which peaks at the maximum depletion of (2,0).

The SA of the (2,0) and (2,1) channels is highlighted by changing the phase of the $1\omega 2\omega$ field by π and subtracting one data set from the other, shown in Fig. 3. Clear asymmetry is seen between the early and late arriving I^{2+} signals coming from the (2,0) channel, resulting from SA in the depletion of this channel. The depletion of the (2,0) signal must end up in the (2,1) signal and, as the depletion shows SA, the increase in the (2,1) signal should also show SA, as is observed. The remarkable feature of these data is that the SA of the (2,1) signal changes sign relative to the (2,0) signal as a function of pump-probe delay or, correspondingly, R.

The data can be divided into three regions: R_e, R_c, and $R > 2R_c$ (as labeled in Fig. 2). The behavior at R_e is best captured with a single $1\omega 2\omega$ pulse and while the (2,0) dissociation channel is observed, no SA is seen in this signal (not shown). At $R > 2R_c$, the SA of the (2,1) signal is in the opposite direction of the (2,0) asymmetry (Fig. 3). This is easily explained in a one-electron picture: assume the maximum electric field points to the left [Fig. 1(a)]. Then, the left potential well will be the upfield well (for an electron). If the two electrons start out in the left well, which we will designate as (0,2), this configuration will be preferentially ionized over the (2,0) configuration, where the two electrons are on the right. The (0,2) configuration will be depleted relative to the (2,0) and the (2,0) signal will dominate. At the same time, the (0,2) configuration will ionize to the (1,2), which will, in turn, dominate over the (2,1). So, the (2,0) and (1,2) signals will be the largest and the I^{2+} ions will come out in opposite directions, as is seen at large R (400 fs) in Fig. 4.

Finally, at R_c, the situation is quite different. As before, the (0,2) configuration will be preferentially ionized, leaving the (2,0) signal stronger than the (0,2). As expected, this aspect is independent of R as seen by the relatively constant asymmetry in Fig. 3. However, at the same time, we find that the (2,1) signal is stronger than the (1,2). The only way this is possible is if the (0,2) configuration ionizes to the (2,1). This must involve a two-electron process: one of the electrons on the left ionizes while the second electron transfers to the right well [Fig. 1(b)]. This additional charge transfer step cannot be detected with a spatially symmetric (1ω) pulse. A direct comparison of the SA observed at 170 fs ($\sim R_c$) and 400 fs ($\sim 2R_c$) is given in Fig. 4.

Given the counterintuitive nature of this last observation, we solved the time-dependent Schrödinger equation (TDSE) through the wave packet propagation of two electrons in a one-dimensional double-well soft Coulomb potential for a model molecular ion A_2^{2+} in an asymmetric $1\omega 2\omega$ field [21,37–39]. Within this model, electron correlation is included exactly. The two-electron wave function is spatially symmetric resulting in singlet states only. A pulse duration of 10 fs was used, but runs with longer pulse durations exhibited qualitatively similar results. We kept the maximum field direction constant (to the left) and calculated the total ionization probability for the (2,0)

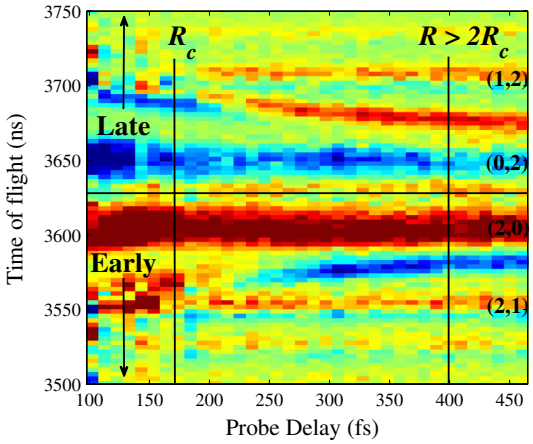

FIG. 3 (color online). Difference between I^{2+} signals when the $1\omega 2\omega$ phase ϕ is rotated by π showing the spatial asymmetry (SA) as a function of probe delay. Red is positive signal and blue is negative. The vertical lines correspond to 170 fs ($\sim R_c$) and 400 fs ($\sim 2R_c$).

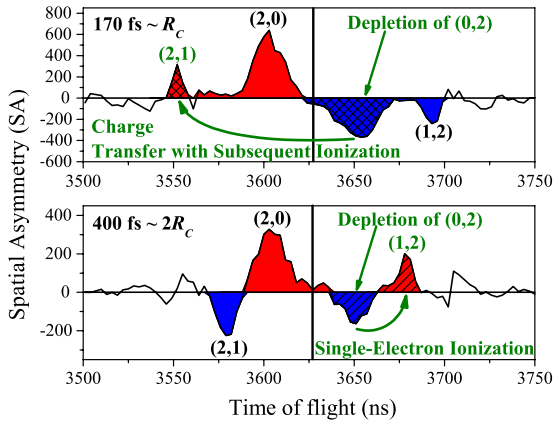

FIG. 4 (color online). Spatial asymmetry for I^{2+} for probe delays of 170 and 400 fs as noted in Fig. 3. The SA of (2,1) at 170 fs (top) is in the same direction as (2,0), while the SA of (2,1) at 400 fs (bottom) is in the opposite direction of (2,0). The curved arrows indicate the ionization pathways based on the depletion of (0,2). Near R_c the depletion of (0,2) corresponds to an enhancement of (2,1). As R increases beyond R_c the depletion of (0,2) corresponds to an enhancement of (1,2).

and (0,2) configurations. An absorbing region is placed around the edge of the spatial grid to simulate ionization. Single electron ionization is characterized by one electron coordinate becoming large while the other coordinate remains small. When one electron reaches the absorber, we record the position of the second, still bound electron, to determine which well it is left in. This information is plotted around the edges of the grids in Fig. 5. We are then able to observe the two-electron wave function evolution as a function of time for various R while monitoring the ionization.

The results of the simulations are given in Fig. 5 for two different R values at the beginning, peak and end of the laser pulse. The peak electric field is shown in Figs. 5(b) and 5(e) pointing to the left in the direction of the upfield well. The two-electron wave function is initially placed in the upfield well of the molecule as shown in Figs. 5(a) and 5(d). We also ran the simulations for ionization in the downfield well. The ionization probability of the molecule is identified by absorption at the grid boundary as shown in Figs. 5(b), 5(c), 5(e), and 5(f) and allows us

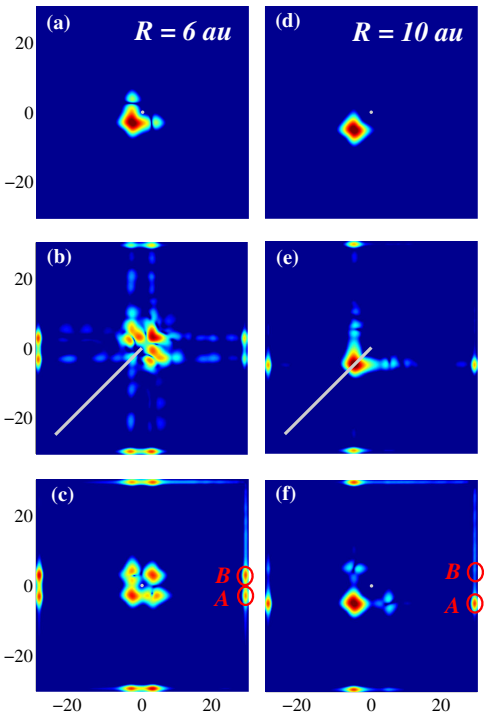

FIG. 5 (color online). Simulation results for the two-electron wavefunction probability densities (plotted on log scale) initially placed in the upfield well (0,2) at $R = 6$ and 10 au (a), (d) prior to the pulse, (b), (e) at the peak of the pulse, and (c), (f) at the end of the pulse. The bar in (b) and (e) represents the peak electric field strength and direction. The ionization probabilities are circled in (c) and (f) showing single-electron ionization (A) and ionization with charge transfer (B) where A and B are defined in Eq. (1). The axes are the coordinates of the two electrons in atomic units. The peak electric field is 0.05 au ($I \approx 9 \times 10^{13}$ W/cm^2) and the pulse duration is 10 fs.

to see which ionization pathway [described by Eq. (1)] is dominant as a function of R. In this figure, ionization leaving the bound electron with a positive coordinate requires electron transfer in addition to ionization.

The values of $R = 6$ and 10 au correspond qualitatively to small (between $\sim R_c$ and $2R_c$) and large R ($R > 2R_c$), respectively. In both trials of R, the (0,2) configuration had a greater ionization probability than the (2,0), consistent with the observed constant SA in the (2,0) channel in Fig. 3. We find that for $R = 10$ au (Figs. 5(d)–5(f)), single-electron ionization is dominant from the upfield well as the ionization probability found at the absorber in Fig. 5(f) is much higher at A than at B [A and B are as defined in Eq. (1)]. The (0,2) channel is ionized to the (1,2) and is in agreement with the observations of EI in which the upfield well ionizes more strongly than the downfield well. Here, the 2^+ ion helps the laser to ionize the upper well. If the molecule starts in the downfield well, the 2^+ ion works against the field and inhibits ionization. The large separation of the nuclei results in a broad internal barrier such that electron localization occurs in the upfield well and any two-electron effects become negligible. Thus, at large R, the bound electron stays in the same well as was initially populated [Fig. 5(f)]. At $R = 6$ au or equivalently, the region around R_c, (0,2) is still ionized more strongly than (2,0), but ends up as (2,1) more often than (1,2). As shown in Figs. 5(a)–5(c), there is a large amount of electronic charge transfer between the upfield and downfield wells of the molecule. In fact, this two-electron charge transfer is the dominant mechanism through which ionization proceeds. The ionization probability found at the absorber boundary is actually larger for the ionization with charge transfer pathway [B in Fig. 5(c)] than for the single-electron ionization pathway [A in Fig. 5(c)] and leaves the remaining electron in the opposite well. Close inspection of the time-dependent calculations suggest that the covalent ground state (1,1) is first strongly populated, moving one electron across the molecule. Then, the upper well is further ionized leading to the counterintuitive (2,1) channel. It should be noted that this two-electron effect is observed in the simulations even with a symmetric laser field. The simulations support the experimental results shown in Fig. 4 where strong electronic charge transfer is the mechanism responsible for the observed SA of (2,0) near R_c.

Our results impact the interpretation of two previous experiments: observations of SA in N_2 [27] and measurements of EI in I_2 [12]. It has been suggested that the SA in N_2 is produced at R_c. This is reasonable as our previous work [28] shows that (2,0) can be produced asymmetrically at R_c. However, the N_2 molecule does not expand to R_c until *after* N_2^{2+} is created [34]. Since the N_2^{2+} molecule is created before expansion to R_c, the (2,0) channel must first be created spatially symmetric near R_e. Based on our new measurements, we propose that the observed SA comes

from the spatially asymmetric depletion of (2,0) once it moves through R_c. However, EI and EL were originally discussed as one-electron effects where (2,0) would ionize to (2,1) and not (1,2) although these two possibilities, the latter being a two-electron effect, could not be distinguished without a $1\omega 2\omega$ field. This description would lead to (2,0) and (2,1) coming out in opposite directions, based on measurements of the I^{2+} ion. The results of our experiment and simulations indeed show that at large R, two-electron effects are negligible and single electron ionization is an accurate description of the dynamics such that (2,0) ionizes to (2,1), consistent with [12]. However, the single electron description gives the wrong directions based on observations of N_2, where (2,0) and (2,1) come out in the same direction. Our conclusions based on the measurements of I_2 and simulations near R_c are actually consistent with observations in N_2 as the strong two-electron charge transfer results in counterintuitive ion yields and the (2,0) and (2,1) are in the same direction. Therefore, two-electron charge transfer must be the mechanism by which (2,0) is asymmetrically depleted near R_c and ionized to (1,2).

In conclusion, we have directly observed multielectron effects both experimentally and theoretically in the asymmetric depletion of the (2,0) channel of I_2^{2+}. The dynamics of two-electron charge transfer produce the dominant pathway for ionization of the molecule at small internuclear separations around R_c. As R gets larger and the molecule expands, the two-electron effects become negligible and the one-electron description of EI sufficiently describes the ionization dynamics.

We would like to acknowledge support from the NSF under Grant No. PHYS-0968799.

[1] E. Gagnon, P. Ranitovic, X. Tong, C. L. Cocke, M. M. Murnane, H. C. Kapteyn, and A. S. Sandhu, Science **317**, 1374 (2007).
[2] B. K. McFarland, J. P. Farrell, P. H. Bucksbaum, and M. Gühr, Science **322**, 1232 (2008).
[3] W. Li, X. Zhou, R. Lock, S. Patchkovskii, A. Stolow, H. C. Kapteyn, and M. M. Murnane, Science **322**, 1207 (2008).
[4] H. Akagi, T. Otobe, A. Staudte, A. Shiner, F. Turner, R. Dörner, D. M. Villeneuve, and P. B. Corkum, Science **325**, 1364 (2009).
[5] M. Kotur, T. C. Weinacht, C. Zhou, and S. Matsika, Phys. Rev. X **1**, 021010 (2011).
[6] H. Chen, V. Tagliamonti, and G. N. Gibson, Phys. Rev. Lett. **109**, 193002 (2012).
[7] P. B. Corkum, Phys. Rev. Lett. **71**, 1994 (1993).
[8] A. D. Bandrauk and H. Z. Lu, Phys. Rev. A **68**, 043408 (2003).
[9] Y. Mairesse, J. Higuet, N. Dudovich, D. Shafir, B. Fabre, E. Mével, E. Constant, S. Patchkovskii, Z. Walters, M. Yu. Ivanov, and O. Smirnova, Phys. Rev. Lett. **104**, 213601 (2010).
[10] T. Seideman, M. Y. Ivanov, and P. B. Corkum, Phys. Rev. Lett. **75**, 2819 (1995).
[11] T. Zuo and A. D. Bandrauk, Phys. Rev. A **52**, R2511 (1995).
[12] E. Constant, H. Stapelfeldt, and P. B. Corkum, Phys. Rev. Lett. **76**, 4140 (1996).
[13] D. Pavičić, A. Kiess, T. W. Hansch, and H. Figger, Phys. Rev. Lett. **94**, 163002 (2005).
[14] I. Bocharova, R. Karimi, E. F. Penka, J.-P. Brichta, P. Lassonde, X. Fu, J.-C. Kieffer, A. D. Bandrauk, I. Litvinyuk, J. Sanderson, and F. Légaré, Phys. Rev. Lett. **107**, 063201 (2011).
[15] E. Lötstedt, T. Kato, and K. Yamanouchi, Phys. Rev. A **85**, 041402(R) (2012).
[16] H. Chen, L. Fang, V. Tagliamonti, and G. N. Gibson, Phys. Rev. A **84**, 043427 (2011).
[17] J. P. Nibarger, M. Li, S. Menon, and G. N. Gibson, Phys. Rev. Lett. **83**, 4975 (1999).
[18] C. Guo, M. Li, and G. N. Gibson, Phys. Rev. Lett. **82**, 2492 (1999).
[19] J. H. Posthumus, K. Codling, L. J. Frasinski, and M. R. Thompson, Laser Phys. **7**, 813 (1997).
[20] G. N. Gibson, M. Li, C. Guo, and J. P. Nibarger, Phys. Rev. A **58**, 4723 (1998).
[21] K. Harumiya, H. Kono, Y. Fujimura, I. Kawata, and A. D. Bandrauk, Phys. Rev. A **66**, 043403 (2002).
[22] H. Yu and A. D. Bandrauk, Phys. Rev. A **56**, 685 (1997).
[23] L. Torlina, M. Ivanov, Z. B. Walters, and O. Smirnova, Phys. Rev. A **86**, 043409 (2012).
[24] W. Li, A. A. Jaroń-Becker, C. W. Hogle, V. Sharma, X. Zhou, A. Becker, H. C. Kapteyn, and M. M. Murnane, Proc. Natl. Acad. Sci. U.S.A. **107**, 20 219 (2010).
[25] B. Sheehy, B. Walker, and L. F. DiMauro, Phys. Rev. Lett. **74**, 4799 (1995).
[26] S. De *et al.*, Phys. Rev. Lett. **103**, 153002 (2009).
[27] K. J. Betsch, D. W. Pinkham, and R. R. Jones, Phys. Rev. Lett. **105**, 223002 (2010).
[28] V. Tagliamonti, H. Chen, and G. N. Gibson, Phys. Rev. A **84**, 043424 (2011).
[29] S. V. Menon, J. P. Nibarger, and G. N. Gibson, J. Phys. B **35**, 2961 (2002).
[30] J. Breidbach and L. S. Cederbaum, Phys. Rev. Lett. **94**, 033901 (2005).
[31] O. Smirnova, Y. Mairesse, S. Patchkovskii, N. Dudovich, D. Villeneuve, P. Corkum, and M. Y. Ivanov, Nature (London) **460**, 972 (2009).
[32] S. Patchkovskii, Z. Zhao, T. Brabec, and D. M. Villeneuve, Phys. Rev. Lett. **97**, 123003 (2006).
[33] A. E. Boguslavskiy, J. Mikosch, A. Gijsbertsen, M. Spanner, S. Patchkovskii, N. Gador, M. J. J. Vrakking, and A. Stolow, Science **335**, 1336 (2012).
[34] J. P. Nibarger, S. V. Menon, and G. N. Gibson, Phys. Rev. A **63**, 053406 (2001).
[35] W. C. Wiley and I. H. McLaren, Rev. Sci. Instrum. **26**, 1150 (1955).
[36] G. N. Gibson, R. N. Coffee, and L. Fang, Phys. Rev. A **73**, 023418 (2006).
[37] G. N. Gibson, Phys. Rev. A **67**, 043401 (2003).
[38] I. Kawata, H. Kono, Y. Fujimura, and A. D. Bandrauk, Phys. Rev. A **62**, 031401(R) (2000).
[39] G. Camiolo, G. Castiglia, P. P. Corso, E. Fiordilino, and J. P. Marangos, Phys. Rev. A **79**, 063401 (2009).